Experimental Study of Feasibility in Kinetically-Controlled Reactive Distillation

Madhura Chiplunkar, Mooho Hong, Michael F. Malone, and Michael F. Doherty
Dept. of Chemical Engineering, University of Massachusetts, Amherst, MA 01003

DOI 10.1002/aic.10302
Published online in Wiley InterScience (www.interscience.wiley.com).

Bifurcation studies predict limited ranges of feasibility for products in certain reactive distillations. These are closely related to the bifurcations in the singular points of dynamic models for simple reactive distillation (isobaric open evaporation with liquid phase reaction). A new dynamic model is described with constant vapor rate together with an experimental study for the reactive distillation of acetic acid with isopropanol to produce isopropyl acetate, catalyzed by Amberlyst-15 ion-exchange resin. An experimental apparatus with real-time measurement of liquid compositions based on Fourier transform infrared (FTIR) spectroscopy is described, and used to follow the composition dynamics at several initial conditions and Damköhler numbers (Da). The experimental results match model predictions that show four regions of behavior. For Da $\approx$ 1*, these show a stable node at acetic acid and several other fixed points as saddles. However, near Da* $\approx$ 2*, both isopropanol and acetic acid are stable nodes and a quaternary singular point appears. The presence of two stable nodes requires the presence of a distillation boundary and, therefore, a limited feasibility for the bottom product compositions from continuous reactive distillation. For the reaction rates studied, the model predictions are closely consistent with the experimental findings, and are robust to variations in the vapor rate. These experiments are among the first to analyze the dynamics and feasibility in a kinetically-controlled reactive distillation and are consistent with previous studies for the reaction equilibrium limit, indicating the formation of a reactive azeotrope.* © 2005 American Institute of Chemical Engineers *AIChE J,* 51: 464–479, 2005
Keywords: kinetically-controlled reactive distillation, feasibility, isopropyl acetate reaction, infrared spectroscopy

Introduction

Reactive distillation is a process alternative that combines reaction and distillation into a single device. Examples of successful reactive distillations are the methyl acetate process, invented by the Eastman Chemical Company (Agreda and Partin, 1984; Agreda et al., 1990) and the diphenyl carbonate process at GE plastics (Oyevaar et al., 2000). However, combining reaction and distillation is not always advantageous, and in some cases may not even be feasible. For example, temperatures for reaction and phase equilibrium may have a large mismatch, some systems may have large energy requirements and costs, for example, ethylene glycol reactive distillation (Okasinski and Doherty, 1997), or interactions of phase behavior and reactions may make separations difficult (Doherty and Malone, 2001). Thus, it is necessary to decide whether reactive distillation is a good alternative and a general set of rules is necessary to decide feasibility and incentives for reactive distillation (Xu et al., 1985; Bessling et al., 1998). The feasible product compositions from a reactive distillation are deter-

Correspondence concerning this article should be addressed to M. F. Doherty at this current address: Dept. of Chemical Engineering, UCSB, Santa Barbara, CA 93106; e-mail: mfd@engineering.ucsb.edu.
This article includes Supplementary Material available from the authors upon request or via the Internet at http://interscience.wiley.com/jpages/0001-1541/suppmat.

mined for a given feed, column pressure and a rate of reaction, which can be varied parametrically to enlarge the design space (Doherty and Malone, 2001). To design a reactive distillation column, it is necessary to know the product composition specifications that generate a feasible column design and how they depend on operating conditions. Thus, once the basic process chemistry and phase equilibrium are known, feasible product compositions can be obtained from theory (Chadda et al., 2001) and be used in design. However, the validity of this new feasibility theory needs to be tested, suggesting the need for experiments.

Depending on the rates of reaction in a column three reaction regimes can be defined, extremely slow reaction rate, intermediate or finite rates of reaction (kinetically-controlled reaction regime), and very fast reaction (chemical equilibrium limit). Feasibility theory has been developed for all three cases. At the no reaction limit, Stichlmair and Herguijuela (1992), Wahnschafft et al. (1992), and Fidkowski et al. (1993) used pinch-tracking methods, to calculate feasible products in conventional distillation columns. For large rates of reaction, at the limit where chemical equilibrium is approached, the effects of chemical reaction have been captured using residue curve maps and pinch tracking methods (Barbosa and Doherty, 1988a,b; Espinosa et al., 1995; Ung and Doherty, 1995a,b). Operation near reaction equilibrium may not be desirable because of the high residence times, large catalyst requirements, and large holdups. Thus, the studies at finite rates of reaction are important, which also include the effects of chemical kinetics on feasibility.

There are various theoretical approaches available that capture effects of finite reaction rates, for example, static analysis methods (Giessler et al., 1998, 1999; Lee et al., 2000), residue curve/bifurcation analysis methods (Rev, 1993; Venimadhavan et al., 1994, 1999; Thiel et al., 1997; Chadda et al., 2000, 2001). However, there have not been experiments aimed at studying feasibility in the kinetically-controlled reaction regime. Some experimental studies have been performed near reaction equilibrium. Song et al. (1997) proved the existence of a reactive azeotrope in the isopropyl acetate reaction system at the limit approaching chemical reaction equilibrium. In another study, Song et al. (1998) determined the effects of heterogenous kinetics in methyl acetate synthesis and measured the residue curve map close to reaction equilibrium. Many experiments studying reaction rates, phase and reaction equilibria, adsorption equilibria for heterogeneous catalysts, selectivity and mass transfer have been reported but none have been directed at testing feasibility theory for reactive distillation. This article validates the feasibility theory proposed by Chadda et al. (2001) for reaction rates that lie in the kinetically-controlled reaction regime.

The algorithm proposed by Chadda et al. (2001) is based on a bifurcation analysis to predict feasible distillate and bottom products at all reaction rates. They represent each section in a distillation column by a cocurrent isobaric flash cascade, as shown in Figure 1a. They have demonstrated that the feasible splits predicted from a bifurcation analysis of the fixed points of the flash-cascade model are in good agreement with the predictions from column simulations. Thus, the algorithm can be used effectively to quickly estimate the sharp splits from a continuous reactive distillation column. In the kinetically-controlled reaction regime the fixed-point criteria are different for the rectification and stripping cascades. They showed that the fixed points for simple reactive distillation are equivalent to the fixed points for a stripping cascade and provide information about potential bottoms from a column. Information about potential distillates from a column can be obtained from the fixed points of a rectifying cascade. The feasibility diagram shows the feasible products to be expected from a continuous column at any rate of reaction.

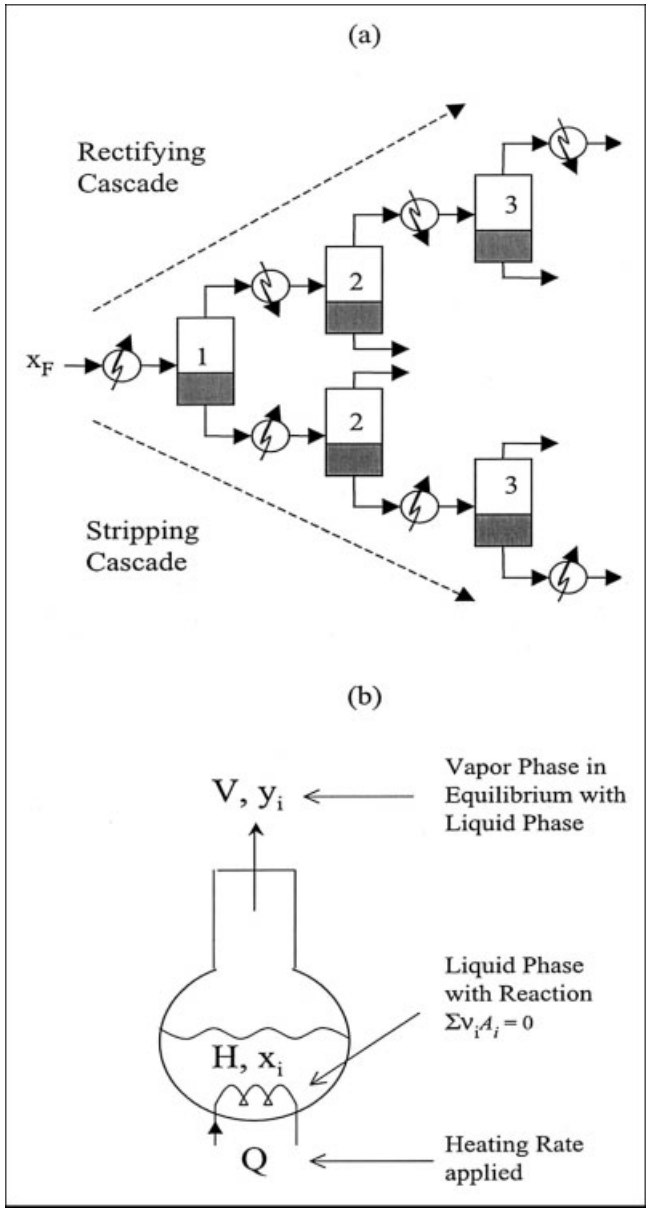

Figure 1. (a) Cocurrent flash-cascade arrangement (Chadda et al., 2001), and (b) Simple reactive distillation still.

This research describes an experimental study of the stripping section of a reactive distillation column that was performed by means of a simple open evaporation apparatus

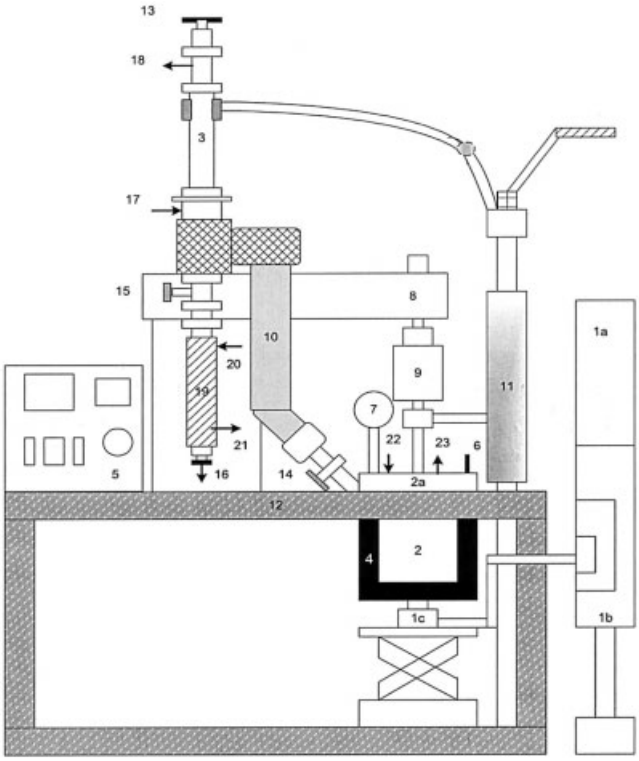

Figure 2. Experimental apparatus.

(Figures 1b and 2). We also describe the development of a model that explains the composition changes in the reaction system.

Isopropyl Acetate System

The esterification of acetic acid to isopropyl acetate was chosen as a model system for investigation. Isopropyl acetate is made by the liquid-phase reaction between isopropanol and acetic acid, using acidic catalysts, such as sulfuric acid or sulphonic acid ion-exchange resin (Amberlyst-15, Rohm and Haas Co., PA). The physical property data for the four components are given in the Supporting Information in Tables PP-1 and PP-2. The reaction chemistry is given by

$$Isopropanol(IPOH) + Acetic\ Acid\ (HOAc) \rightleftharpoons Isopropyl\ Acetate\ (IPOAc) + Water(H_2O) \quad (1)$$

At elevated temperatures of 120°C or higher over an Amberlyst-15 catalyst, side reactions occur in which isopropanol dehydrates to form diisopropyl ether, propylene, and water (Heese et al., 1999). Such side reactions were not considered in this study because the reactor rarely reached this temperature level. The catalyst used, Amberlyst-15, is a macroreticular ion-exchange resin that is an ensemble of microspheres of size 250 Å. More than 95% of all the protons are inside the microspheres and are accessible only to the components that are able to penetrate the network of polymer chains and are able to adsorb at the catalyzing sites. Since adsorption effects are present in the system and diffusion is fast within the catalyst (Thiel et al., 1997), the Langmuir-Hinshelwood-Hougen Watson (LHHW) kinetic rate model is used (Kipling, 1965) without accounting for mass transfer limitations within the catalyst.

The reaction rate is given by the LHHW model (Manning, 1999) as

$$r = \frac{k_s\left(a_{IPOH}a_{HOAc} - \frac{1}{K_{eq}}a_{IPOAc}a_{H_2O}\right)W}{(1 + K_{HOAc}a_{HOAc} + K_{IPOH}a_{IPOH} + K_{IPOAc}a_{IPOAc} + K_{H_2O}a_{H_2O})^2} \quad (2)$$

where r is the reaction rate in mol reacted [mol of mixture]$^{-1}$ min^{-1}, a_i is the activity of the component i, and W is the concentration of catalyst in the reacting liquid mixture in mol H^+/mol of mixture. K_i is the component adsorption equilibrium constant for species i and K_{eq} is the thermodynamic reaction equilibrium constant for the isopropyl acetate reaction. The apparent forward reaction rate constant k_s as a function of temperature is given by

$$k_s = k_s^0 e^{(-E/RT)} \quad (3)$$

where E is the activation energy for the reaction. An equilibrium constant of $K_{eq} = 8.7$ was taken from the literature (Lee and Kuo, 1996). This value of K_{eq} is independent of temperature measured over the boiling temperature range of the mixture at atmospheric pressure. The kinetic parameters (the kinetic rate constant and adsorption equilibrium constants) for the LHHW model were obtained by regression of the kinetic data reported by Manning (1999) and reported here in Table 1.

Liquid-phase nonideality has been accounted for by using the NRTL model to determine activity coefficients. The thermodynamic equations and constants used are listed in Table PP-3 in Supplementary Material (Supporting Information). Component vapor pressures were calculated using the Antoine equation. Species constants and binary interaction parameters were taken from the DECHEMA series (Gmehling and Onken, 1977). For the water-isopropyl acetate pair, only azeotrope data could be obtained. NRTL parameters for this pair were estimated using the UNIFAC estimation technique by Manning (1999). Acetic acid dimerizes in the vapor phase and vapor-phase association is incorporated directly into the phase equi-

Table 1. Reaction Rate Constant and Adsorption Equilibrium Constants (Manning, 1999)

Adsorption Equilibrium Constants, K_i	
Components	K_i
Isopropanol (1)	0.23961
Isopropyl Acetate (2)	0.147
Water (3)	0.50797
Acetic Acid (4)	0.19766
Reaction Rate Constants, in (mol reacted [mol H^+]$^{-1}$ min^{-1})	
$k_s = 2.2 \times 10^{10}\ e^{(-8268.9/T(K))}$	
$K_{s,ref} = 1.065$	
$T_{ref} = 75$°C	

librium equations (Marek and Standart, 1954; Manning, 1999). The dimerization constant parameters for acetic acid dimerization are listed in Table PP-3 in Supplementary Material.

Experiments

Materials

The chemicals used for the experiments are isopropanol (purity >99.5 wt%), acetic acid (purity >99.7 wt%), isopropyl acetate (purity >99 wt%), (Aldrich Chemicals Co., WI), and deionized water. The catalyst used was Amberlyst-15 wet (Rohm and Haas Co., PA). The catalyst properties, as specified by the manufacturer, were as follows: Opaque beads with hydrogen as ionic form with bulk density of 0.7689 g/cm^3 (48 lbs/ft^3), acid site concentration of 4.7 meq H^+/g dry catalyst (4.7×10^{-3} mol H^+/g dry catalyst), minimum moisture holding capacity 52–57 wt% (H^+ form). The surface area and average pore diameter are 45–50 $\times$ 10^4 cm^2/g and 250 Å, respectively. The catalyst can withstand temperatures up to 120°C. The reactor is made of Carpenter-20 material. It is corrosion resistant and capable of withstanding a pressure of 202.6×10^5 Pa (200 atm, as specified by the manufacturer, Parr Reactor Co., IL). The cooling coil and stirrer are made of Hastelloy-C material. The material of the condenser assembly is stainless steel.

Apparatus

The experimental apparatus shown schematically in Figure 2 consists of (1) a reaction analysis device, *ReactIR 1000* (ASI Applied Systems, 1997), (2) a 1,000 ml reactor, and (3) a condenser unit. The reaction analysis device performs composition analysis using Infrared Spectroscopy. It consists of (1a) an optics module which records the infrared spectra, (1b) an electronics module which converts the spectra to compositions by means of a calibration, and (1c) an *in situ* analysis probe to collect real-time compositions. Cooling and heating of the reactor is achieved by using a cooling coil attached to the head of the reactor (2a), and by an external heater assembly (4), respectively. Cooling of the vapor is achieved by means of a condenser assembly (3). Desired temperature is maintained by altering the settings of the digital temperature controller (PARR 4842, Series 989) (5). In order to provide heating, a 150 V AC voltage controller is used (Ace Glass incorporated, CAT 12088-05). This heater (4) is calibrated, using pure isopropanol as the sample, so that the applied voltage is related to the heat supplied. (The voltages applied ranged from 60 to 75 V. The maximum value that can be applied to the heater is 95 V. The range of heating rates possible is ≈2.93 kJ/min for 60 V applied, to ≈11.71 kJ/min for 95 V. However, the experiments are performed at a value of 65 V to prevent quick drying of the still, and to ensure a sufficiently low vapor rate. The heating rate for an applied voltage of 65 V is ≈3.97 kJ/min). The temperature controller is used to maintain a setpoint for the reaction or just to read the temperature (5). A thermowell attached to the head of the reactor fitted with a thermocouple (6) is connected to the controller. A pressure gauge (7) is fitted to the head of the reactor. There is a pressure transducer arrangement in the controller to measure the pressure inside the reactor. A motor assembly (8) provides power to the stirrer or the agitator assembly (9), fitted to the head of the reactor that keeps the heterogeneous catalyst suspended in the liquid. It is possible to regulate the speeds of agitation for the motor. The condenser assembly (3) is attached to the reactor head. To minimize heat losses to the surrounding, insulation (10) is provided over the passage through which the vapor goes to the condenser. The head and the agitator assembly along with the entire condenser assembly is movable with the help of a winch and pulley arrangement (11), whereas a trolley and frame support the entire assembly (12).

Valve (13) maintains the assembly open to atmosphere to maintain atmospheric pressure. Valve (14) allows vapor flow to the condenser. The condenser assembly (3) condenses the vapor which can be refluxed using valve (15) or collected using valve (16). The NESLAB RTE-111 circulator achieves the cooling water circulation for the condenser, as well as the reactor. Cooling water is circulated through lines (17) to (23). The reactants are preheated in a constant temperature bath maintained at a constant temperature using a digital circulator (HAAKE, DC3). Experimental conditions are given in Table 2.

Table 2. Experimental Conditions

Pressure: 1.013×10^5 Pa (atmospheric pressure)
Process Time: ≈ 100 min [H_0/V_0 ≈ (10 mol)/(0.1 mol/min)]
Initial Liquid Volume: ≈ 800 ml
Vapor Rate maintained: $V_0 \approx 0.08 - 0.12$ mol/min
Voltage: 65 V, i.e. $Q \approx 3.97$ kJ/min
Speed of Agitation: ≈ 500–550 rpm

	$Da \approx 1$	$Da \approx 2$
Catalyst:	20–30 g	43–50 g
Initial Catalyst Concentration: (g catalyst/g liquid)	3.7 wt %	7.6 wt %
Reaction Time ($1/k_{s,ref}W_0$):	100 min	50 min
Damköhler Number:	0.84–1.21	1.61–2
Scaled Damköhler Number $D = Da/(1 + Da)$:	0.46–0.55	0.62–0.67
Number of Runs:	54	41

Composition analysis

The instrument used for analyzing the liquid compositions is *ReactIR 1000,* a compact bench top instrument designed for real-time, *in situ* analysis of chemical reactions using Infrared Spectroscopy (refer to Figure 2). The device collects reaction temperature data and the IR spectra (using optics module (1a) and collection probe (1c)), and analyzes the mid-infrared region of the spectra (using electronics module (1b)), which is the molecular fingerprint region of the chemicals. Each spectrum is a Fourier transformation of 256 acquisitions collected over the spectral ranges of 4400–2150 and 1950–650 cm^{-1} with a time period of 2 min, and an instrument resolution of 8 cm^{-1}. A diamond sensor probe is fitted to the bottom of the reactor for mounting of a fiber optic transducer that provides both incident and collected signals for the instrument.

The data are collected as absorbance spectra in real time and are converted to compositions using a calibration. The calibration is made using 100 ml samples of known compositions and temperatures: pure components, binary, ternary and quaternary mixtures are used for this purpose. We used 94 mixtures of known composition for calibration (reported in the Supplemen-

tary Material (Table S-1); Chiplunkar, 2002). After the calibration solution is put into the reactor, it is sealed and pressurized using high purity helium gas (Merriam Graves Co., MA, 4.7, 1071–300 with a minimum purity of 99.997 vol%) to about 6.2×10^5 Pa (90 psi) to prevent boiling. Spectra are taken in the temperature range 25–120°C. The *QuantIR* software (ASI Applied Systems, 1997) uses the factor analysis method (Kramer, 1998) to produce a regressed calibration of absorbance vs. composition. In order to evaluate the calibration, evaluation samples were used, using compositions different from those used in the calibration. An average of the compositions measured over the collection time for each component, and the known compositions is taken. The disparity between the measured and actual compositions is calculated from the absolute error given as

$$\text{Absolute Error} = |x_{\text{known}} - x_{\text{measured}}| \tag{4}$$

where, x_i is the mole fraction of each component. Both average and maximum absolute measurement errors for each sample are available as Supplementary Material (Table S-2). These errors for the evaluation samples provide an estimate of the errors that can be expected in the main experimental composition data. As seen from the errors in compositions of evaluation samples, the IR instrument, based on the calibration, is capable of distinguishing one part in a hundred. The mole fraction compositions are reported to three decimal places but they are only accurate up to two.

Model

The effects of kinetics on simple reactive distillation have been studied by Solokhin et al. (1990), Venimadhavan et al. (1994), and Thiel et al. (1997). As the simple distillation proceeds, the liquid holdup H decreases, however, the mass of catalyst remains the same and does not deactivate in the experiment. This is an important assumption of the new model. The model developed here makes predictions for a simple reactive distillation, considering the effects of changing catalyst concentration as a function of time. This analysis is key to interpreting the experimental data.

Consider a reaction with equimolar chemistry, taking place in the liquid-phase, as shown by the reaction in Eq. 1. There are $c = 4$ components involved in the reaction. The overall mass balance and component balances for species, $i = 1, \ldots, c$, on the still are (a general model for c components and $\Re$ reactions is derived in the Appendix)

$$\frac{d(Hx_i)}{dt} = -Vy_i + \nu_i r H \tag{5}$$

$$\frac{dH}{dt} = -V \tag{6}$$

where H is the molar liquid holdup, V is the molar vapor rate, x_i and y_i are the liquid and vapor phase mole fractions, respectively, ν_i is the stoichiometric coefficient for component i, and r is the reaction rate, given by Eq. 2. The overall reaction rate is affected by the change of catalyst concentration for homogeneous or heterogeneous catalysts. We define a dimensionless catalyst concentration (W) as the ratio of moles of H^+ to the molar liquid holdup of the mixture

$$W = \frac{M_{cat}}{H}\left(\frac{\text{mol } H^+}{\text{mol of mixture}}\right) \tag{7}$$

where, M_{cat} is the total mol of H^+ of catalyst, which is a product of the acid site concentration (4.7×10^{-3} mol H^+/g dry catalyst) and mass of dry catalyst ($g_{cat}[1 - w]$, g_{cat} is mass of the wet catalyst in g and w is the mass fraction moisture content of catalyst).

Thus, the initial catalyst concentration W_0 is given by

$$W_0 = \frac{(4.7 \times 10^{-3})\, g_{cat}[1 - w]}{H_0}\left(\frac{\text{mol } H^+}{\text{mol of mixture}}\right) \tag{8}$$

The variation of catalyst concentration with time is

$$\frac{dW}{dt} = \frac{d}{dt}\left(\frac{M_{cat}}{H}\right) = -\frac{M_{cat}}{H}\frac{dlnH}{dt} \tag{9}$$

where M_{cat} is a constant. From Eq. 6, $dlnH/dt = -V/H$, and introducing the warped time as $d\xi = (V/H)dt$, we find that the variation of catalyst composition with warped time is exponentially increasing

$$\frac{dW}{d\xi} = W \tag{10}$$

which on integration yields

$$W = W_0 e^{\xi} \tag{11}$$

A dimensionless group, the Damköhler number, is obtained on scaling the equations. This is the ratio of a characteristic process time (H_0/V_0) to a characteristic reaction time $1/(k_{s,ref}W_0)$, where $k_{s,ref}$ is the forward reaction rate constant at a reference temperature of 75°C (see Table 1). Substituting W_0 from Eq. 8

$$Da = \frac{H_0/V_0}{1/(k_{s,ref}W_0)} = \frac{(4.7 \times 10^{-3})\, g_{cat}[1 - w]k_{s,ref}}{V_0} \tag{12}$$

where H_0, V_0 and W_0 are holdup, vapor rate and catalyst concentration, respectively, at the initial time.

Combining the above equations with the rate expression, simplifying, and noting that $(W/W_0)(H/H_0) \equiv 1$, yields the following model

$$\frac{dx_i}{d\xi} = (x_i - y_i) + \nu_i Da\left(\frac{k_s}{k_{s,ref}}\right)\left(\frac{V_0}{V}\right) \times \left[\frac{\left(a_{IPOH}a_{HOAc} - \frac{1}{K_{eq}}a_{IPOAc}a_{H_2O}\right)}{\left(1 + \sum_{i=1}^{4} K_i a_i\right)^2}\right] \quad (13)$$

$$\frac{dH}{d\xi} = -H \quad (14)$$

Depending on the vapor rate policy followed for V_0/V the model (Eqs. 13 and 14) becomes either autonomous or nonautonomous. The enthalpy balance can be used to relate V to V_0

$$\frac{d(h^L H)}{dt} = Q - Vh^V + (-\Delta H_R)rH \quad (15)$$

Heat lost to the surrounding because of convection and radiation is assumed to be constant. The heat input term (Q) is the external heat supplied minus the heat lost to the surrounding. It is assumed that vapor-liquid equilibrium exists at all times, that is, mass transfer between liquid and vapor is faster than composition changes due to reaction, and the temperature is the boiling point of the liquid. Substituting the overall mass balance Eq. 6 and rewriting Eq. 15 in terms of warped time

$$\frac{dh^L}{d\xi} = \frac{Q}{V} - (h^L - h^V) + (-\Delta H_R)Da\left(\frac{k_s}{k_{s,ref}}\right)\left(\frac{V_0}{V}\right) \times \left[\frac{\left(a_{IPOH}a_{HOAc} - \frac{1}{K_{eq}}a_{IPOAc}a_{H_2O}\right)}{\left(1 + \sum_{i=1}^{4} K_i a_i\right)^2}\right] \quad (16)$$

If the enthalpy of the liquid h^L is assumed to be constant with time, Eq. 16 becomes an algebraic equation. Also assuming a constant heat of vaporization λ, implies that $h^V - h^L$ is a constant equal to λ. On simplification the heat balance becomes

$$Q = V\lambda\left(1 - \frac{(-\Delta H_R)}{\lambda}Da\left(\frac{k_s}{k_{s,ref}}\right)\left(\frac{V_0}{V}\right) \times \left[\frac{\left(a_{IPOH}a_{HOAc} - \frac{1}{K_{eq}}a_{IPOAc}a_{H_2O}\right)}{\left(1 + \sum_{i=1}^{4} K_i a_i\right)^2}\right]\right) \quad (17)$$

Or vapor rate can be written as

$$V = V_0\left(\frac{Q}{V_0\lambda} + \left(\frac{-\Delta H_R}{\lambda}\right)Da\left(\frac{k_s}{k_{s,ref}}\right) \times \left[\frac{\left(a_{IPOH}a_{HOAc} - \frac{1}{K_{eq}}a_{IPOAc}a_{H_2O}\right)}{\left(1 + \sum_{i=1}^{4} K_i a_i\right)^2}\right]\right) \quad (18)$$

Knowing the vapor rate desired, the heat to be applied can be calculated, or vice versa. Some theoretical studies of vapor rate policies have been reported previously (Solokhin et al., 1990; Venimadhavan et al., 1994; Martella, 1998).

The important parameters that affect the vapor rate are the Damköhler Number, the heat utilization factor ($-\Delta H_R/\lambda$) (Sundmacher et al., 1994), and the dimensionless heating rate ($Q/V_0\lambda$). For the isopropyl acetate system, the heat of reaction is $\Delta H_R \approx -2.93$ kJ/mol at 75°C (calculated from the heats of formation of components). The average heat utilization factor for the system under consideration is ≈0.08. For reactions with small heats of reaction, or small heat utilization factors, the vapor rate can be maintained constant if the heating rate and the heat of vaporization are constant (Martella, 1998). For the isopropyl acetate reaction chemistry, model calculations show that a constant heating rate thus gives a constant vapor rate. If a changing vapor rate is desired, the heating rate has to be changed according to Eq. 17. A constant heating rate has been implemented in this research, and experimental data corresponding to constant vapor rate are reported.

The composition changes with time can be obtained by integrating Eq. 13 with the policy of constant vapor rate $V = V_0$. The resulting model is autonomous and gives the same solutions as the stripping cascade reported by Chadda et al. (2001). The differential equations are integrated using the LSODES integrator (IMSL/Math Library, 1987). The results are identical to those obtained by Venimadhavan et al. (1994) for a proportional vapor rate (that is, $V/V_0 = H/H_0$), using a model developed with the assumption that catalyst composition remains constant. However, it is difficult to experimentally regulate the heating rate Q as a function of time to maintain this policy; it is also difficult to keep the catalyst concentration constant, which is why we have devised the new experiment.

Bifurcation analysis

Bifurcation studies have been used to classify the various feasible splits as a function of Damköhler Number, Da, or scaled Damköhler number $D = Da/(1 + Da)$. Manning (1999), Venimadhavan et al. (1999), and Chadda et al. (2001) have also performed bifurcation studies of kinetic effects in reactive distillation for the isopropyl acetate system. A bifurcation diagram is a systematic analysis of the steady-state solutions of the component material balances as a parameter is varied. Manning (1999) compared the bifurcation diagrams generated using two different kinetic models (one homogeneous, the other heterogeneous), and showed that they have the

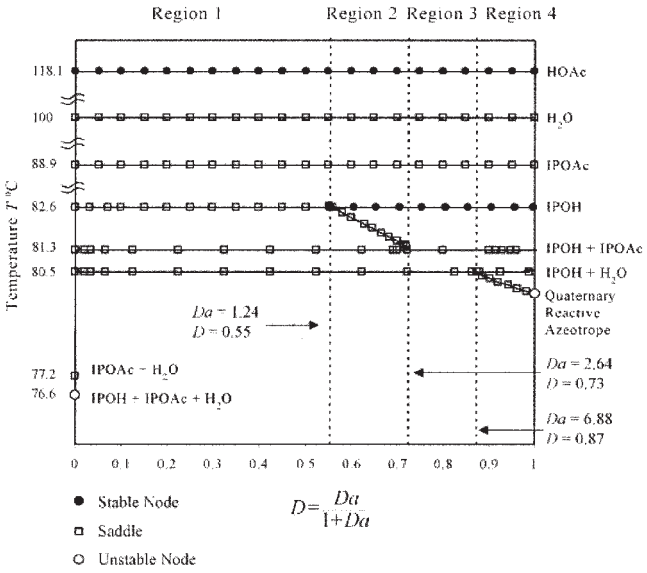

Figure 3. Bifurcation diagram using scaled Damköhler number *D*.

same qualitative features, but the bifurcations occur at different Damköhler numbers.

Single parameter continuation software, AUTO (Doedel, 1986) was used to generate a bifurcation diagram for the steady-state solutions of Eq. 13, with $V = V_0$ (the stripping section bifurcation diagram) for the isopropyl acetate system, Figure 3. For different ranges of Da, different feasible products are obtained. The diagram can be divided into four regions of Damköhler numbers (Regions 1 to 4), each of which has a unique set of features, shown in Figure 3 in this article, and Figure 5 in Chadda et al. (2001). Table 3 lists all the fixed points and their nature predicted for the isopropyl acetate system. All the singular points listed in Table 3 are plotted on the bifurcation diagram in Figure 3. For example, in each of the range of Damköhler numbers between 1.24 and 2.64 (Region 2), and 6.88 and ∞ (Region 4), there are quaternary fixed points predicted as saddles of varying compositions. The pure alcohol branch is a saddle up to $Da = 1.24$, but becomes a stable node beyond it. Thus, a distillation boundary is predicted in Regions 2 and 4. Other branches, such as pure water and isopropyl acetate are predicted to be pure component saddles, whereas isopropanol-water and isopropanol-isopropyl acetate are binary saddles. Acetic acid is a stable node for all Damköhler numbers.

Residue curve maps

Liquid-compositions in reactive distillation can also be represented on residue curve maps (RCM), which are the phase plane of the liquid compositions in an isobaric open evaporation (Barbosa and Doherty, 1988a; Rev, 1993; Venimadhavan et al., 1994; Ung and Doherty, 1995b; Thiel et al., 1997). At reaction equilibrium in a four component mixture, there is a one-to-one relation between the two independent reaction invariants and the three mole fractions. However, representation of compositions by such transformations alone is not sufficient for kinetically-controlled reaction regimes, and a three-dimensional (3-D) representation is necessary. Chadda et al. (2002) found a convenient set of coordinates to represent the liquid-phase compositions using two reaction invariants given by

$$X_1 = x_{HOAc} + x_{IPOAc}, \quad X_2 = x_{IPOH} + x_{IPOAc} \tag{19}$$

together with one reference component mole fraction. X_1, X_2 are the reaction invariants (same as liquid-phase transformed mole fractions) (Ung and Doherty, 1995a), and x_{IPOAc} is the mole fraction of a reference component, isopropyl acetate. A 2-D projection onto the $X_1 - X_2$ plane is also used to explain the results, with the vertices of this square being the four pure component compositions.

Figures 4 and 5 are two such calculated residue curve maps for the system at $Da = 1$ and $Da = 1.86$ in 3-D space represented inside a cube, and its 2-D projection. The tetrahedron drawn in the 3-D figure represents the positive mole fraction, or real composition space. Figure 5 shows a quaternary saddle point, an essential characteristic of Region 2 on the bifurcation diagram. Figure 4 shows no such structure, as predicted for Region 1. These are the key features of the two regions in the kinetically-controlled reaction regime that were tested in the experiments.

Reaction Rate Experiments

After the heat and *ReactIR* calibrations are performed, online measurement of compositions with time can be obtained as the reaction and separation proceeds. The following experimental procedure was followed for a particular reaction rate,

Table 3. Nature of Fixed Points

Fixed Points	Boiling Points (*T*°C)	Nature of Fixed Points	Compositions (liquid mole fraction)
HOAc	118.1	stable node	pure component
H_2O	100.0	saddle	pure component
IPOAc	88.9	saddle	pure component
IPOH	82.6	saddle/stable node	pure component
IPOH + IPOAc	81.3	saddle	0.680 + 0.320
IPOH + H_2O	80.5	saddle	0.667 + 0.333
IPOAc + H_2O (no reaction limit)	77.2	saddle	0.598 + 0.402
IPOH + IPOAc + H_2O (no reaction limit)	76.6	unstable node	0.137 + 0.474 + 0.389
Quaternary (Region 2)	82.7–81.3	saddles	varying compositions
Quaternary (Region 4)	80.5–79.8	saddles	varying compositions
Reactive Azeotrope	79.8	unstable node	0.565 + 0.183 + 0.204 + 0.048[§]

[§]IPOH + IPOAc + H_2O + HOAc.

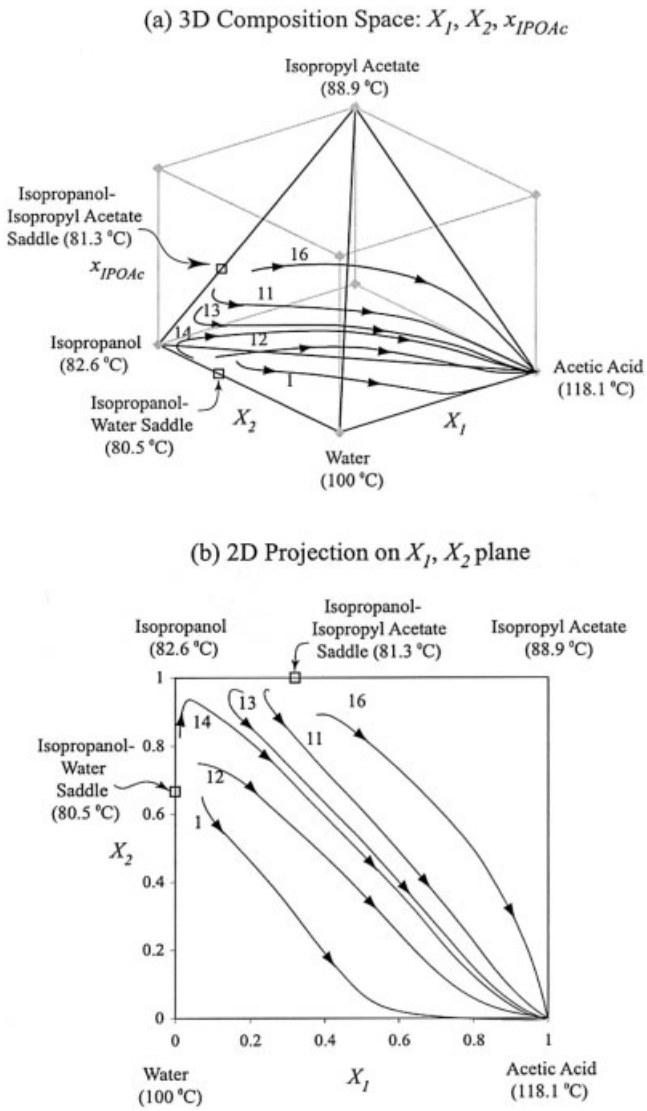

Figure 4. Calculated residue curve map, at *Da* = 1, (a) 3-D composition space, and (b) 2-D projection.

or the selected Damköhler number Da, at which the residue curves were measured (see Chiplunkar (2002) for additional details).

This procedure was followed for each batch. A trajectory (or residue curve) is developed from multiple batches. In order to continue a trajectory, we used the end point composition of the last batch as the starting point of the next, and so on. The condenser was open to the atmosphere, so that a constant atmospheric pressure was maintained. A trajectory consists of anywhere from 4 to 15 runs, each of which were of 10 to 80 min duration, depending on initial composition. For additional details about batches and trajectories refer to Supplementary Material:

(1) To get trajectories on a residue curve map several sets of initial compositions, $x_{i,0}$, need to be chosen. Select $x_{1,0}$, $x_{2,0}$, $x_{3,0}$, $x_{4,0}$, where 1-isopropanol, 2-isopropyl acetate, 3-water, and 4-acetic acid.

(2) Select the constant voltage to be applied (we chose a value of 65 V), which in turn fixes the heating rate (from calibration of Q vs. Voltage).

(3) Calculate the initial vapor rate V_0 from the energy balance, knowing Q and $x_{i,0}$ using Eq. 18. Keep V constant at $V = V_0$.

(4) Measure the mass fraction moisture content of the catalyst (w). Knowing the catalyst acid site concentration, the

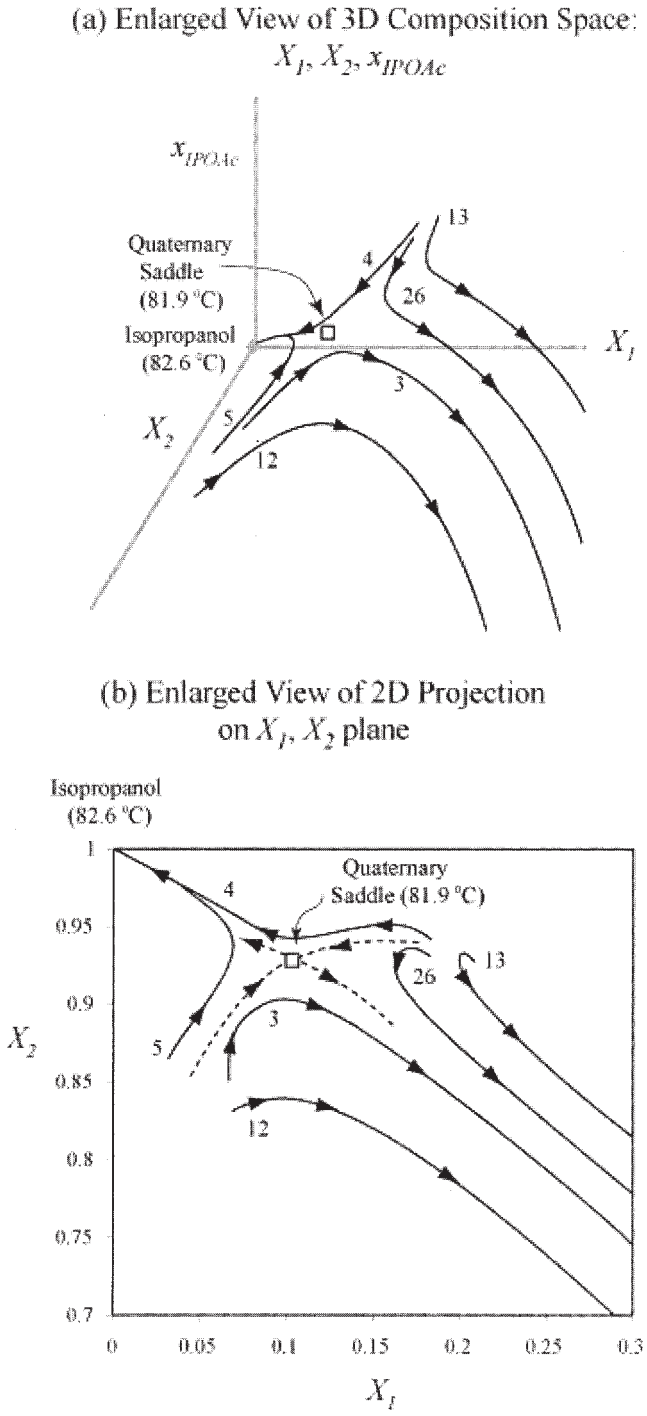

Figure 5. Calculated residue curve map, at *Da* = 1.86, (a) 3-D composition space, and (b) 2-D projection.

selected Damköhler number, the desired vapor rate, and the measured mass fraction moisture content of the catalyst, the grams of catalyst required is calculated using Eq. 12.

(5) Select the initial liquid reactor volume for the experiments (we have chosen ≈800 ml). Calculate the masses of each of the components to be used knowing liquid volume, compositions, densities, and molecular weights of components.

(6) Prior to charging of the reactants, align the FTIR probe (Chiplunkar, 2002).

(7) Mix the two nonreacting components and catalyst and heat them in the reactor under total reflux until a stable temperature of 70°C is reached. The heater supplies the heating rate corresponding to the voltage applied. Heat the other components in a constant temperature waterbath before mixing them in the reactor. Reseal the reactor. This preheating is done to minimize any reaction before the time vapor starts coming out of the reactor (the liquid refluxing time).

(8) Stir the contents of the reactor continuously at a constant speed. The catalyst is suspended in the liquid by agitation. The catalyst is used a single time to eliminate catalyst variability from run to run caused by mechanical breakage due to agitation.

(9) Analyze the liquid compositions (we analyzed the compositions using a precalibrated online liquid composition analysis instrument *ReactIR*).

(10) Condense the vapor distillate and collect the condensed vapor samples every 10 min. Measure the weight of each sample in g and store part of it for composition analysis. From the measured weights and compositions, calculate the average molar vapor rate over the 10 min. (The purpose of measuring the vapor rate was to ensure that composition data corresponding to a constant vapor rate only are chosen). Continue the experiment for the current batch until the vapor rate starts to fall below the constant value, which is found to occur when the molar holdup falls to approximately half its initial value (Figure 6).

(11) After the experiment is over, clean the reactor and condenser.

This procedure was repeated for each batch.

Data Analysis

To implement the experiment, the vapor rate must be maintained constant (that is, $V_0/V = constant$ in Eq. 13. Figures 6a and b show the results of an experiment performed to study the variation of vapor rate with holdup and time, respectively. The experimental conditions were as follows: Damköhler number $Da \approx 2.92$, heating rate $Q = 3.97$ kJ/min, catalyst mass for 30% wet catalyst $g_{cat} = 72.8$ g, and initial holdup $H_0 = 13.5$ mol. The initial compositions in mole fractions were, $x_{IPOH} = 0.694$, $x_{IPOAc} = 0.088$, $x_{H_2O} = 0.214$, and $x_{HOAc} = 0.004$. It is observed that a constant heating rate of $Q = 3.97$ kJ/min is able to give a constant vapor rate of approximately 0.1 mol/min until the molar holdup becomes half its initial value, as marked by the vertical dotted lines in Figure 6. The solid line represents the vapor rate calculated by substituting a constant heating rate of $Q = 3.97$ kJ/min and heat of vaporization λ (values are reported in physical property data Table PP-1 in Supplementary Material) in Eq. 18. From the calculations, vapor rate is found to be almost constant. It can be concluded

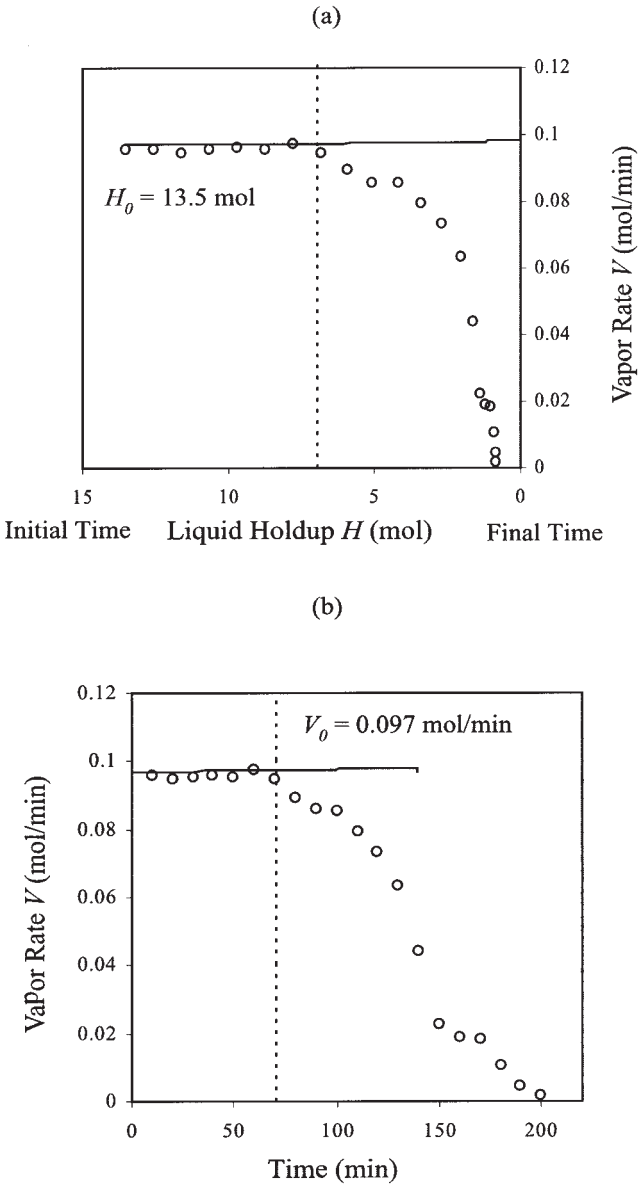

Figure 6. Variation of vapor rate with (a) holdup, and (b) time, for *Da* = 2.92.

Solid lines represent the model predictions, Eq. 18.

that for a reaction with a low-heat utilization factor (such as the isopropyl acetate reaction chemistry), a constant heating rate gives a constant vapor rate until the liquid molar holdup reaches approximately half its initial value and vice-versa, for a constant heat of vaporization (Martella, 1998; Chiplunkar, 2002). The experimental vapor rates obtained for $Da \approx 1$ and $Da \approx 2$ are plotted in Figure 7. Each point corresponds to the time average taken for each run during the period where the vapor rate is constant for that run. The solid lines represent the average taken over all the runs at a fixed Damköhler number. This average vapor rate was used in the calculations. There is some variation in the vapor rates about the average value. Hence, there is a variation in the Damköhler number, that is, at $Da \approx 1$, the maximum and minimum values of Da across all

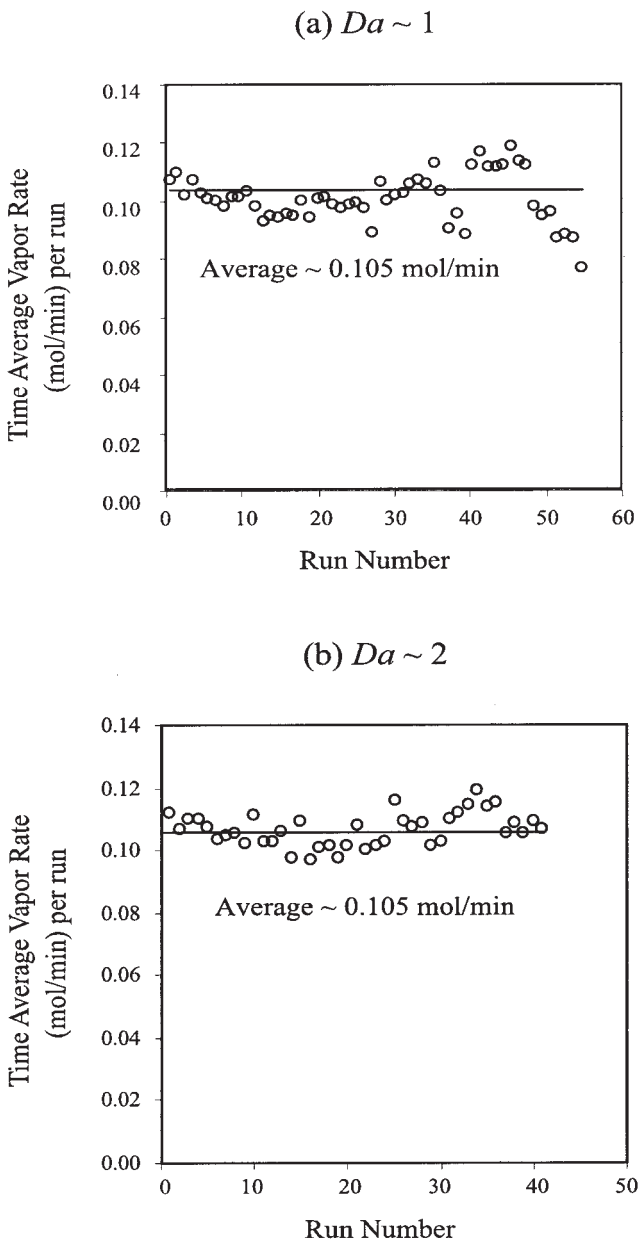

Figure 7. Time averaged vapor rates obtained per run (open circles) for: (a) 54 runs at *Da* ≈ 1, and (b) 41 runs at *Da* ≈ 2.

Solid lines represent average over all runs at (a) $Da \approx 1$ and (b) $Da \approx 2$.

the runs, are 1.21 and 0.84, respectively, whereas at $Da \approx 2$, they are 2 and 1.61, respectively (Table 2). Even with these variations, the Damköhler number belongs to the same region of the bifurcation diagram.

Experimental observations

Figures 8 and 9 show the data obtained for the two reaction rates studied $Da \approx 1$ and $Da \approx 2$, in Regions 1 and 2 of the bifurcation diagram, respectively. The experimental data are shown by the colored points whereas the calculated trajectories are shown as solid lines, with arrows pointing in the direction of increasing time. The calculated trajectories were obtained by integrating Eq. 13 from the experimentally measured initial compositions with $V_0/V \equiv 1$ and using a constant value of *Da*. Table 4 reports the experimental values of initial mole fractions of the first runs of each trajectory at the two Damköhler numbers. Liquid-phase compositions measured online are in mole fractions, and the corresponding reaction invariants are plotted, using Eq. 19. The following quantities are reported in Tables S-3 and S-4 in Supplementary Material, for the two Damköhler numbers, respectively: Initial catalyst concentration (W_0), initial mass of catalyst (g_{cat}), mass fraction moisture content of the catalyst (w), initial molar liquid holdup (H_0), and average vapor rate per run (V_0). The data corresponding to the vapor-phase are obtained by analyzing the condensed vapor samples. Vapor samples are collected every 10 min (Chiplunkar (2002) reports the average vapor masses, cup-mixed average vapor-phase mole fractions ($\bar{y}_i$), and average vapor rates (V) for average values over each 10 min interval).

A total of 54 runs were conducted to generate the phase plane for $Da \approx 1$, for the six trajectories measured, 16, 11, 13, 14, 12, and 1. A total of 41 runs were conducted to generate the phase plane at $Da \approx 2$, for the six trajectories measured, 4, 5, 13, 26, 3, and 12. The following observations were made from the experimental data obtained.

Damköhler number Da ≈ 1

At this reaction rate, a single stable node is predicted at acetic acid, and a pure component saddle is predicted at isopropanol (Figures 3 and 4). There is no prediction of a quaternary fixed point of any kind (Figures 3 and 4). For all the initial compositions, the trajectories were observed to move eventually towards acetic acid. In Figure 8, trajectories 13 and 14 move initially in a direction towards isopropanol, and then move away from it, which is consistent with the prediction that isopropanol is a saddle. Experiments performed near the binary edges of the composition space show that the trajectories move away from the binary azeotropes and pure isopropanol.

Experiments performed near the acetic acid corner of the diagram showed that the still composition gets enriched in acetic acid. Thus, the experimental data are consistent with the prediction of acetic acid being a stable node that can be observed as a bottoms product from a column (Chadda et al., 2001). The experimental data were also found to be consistent with the theoretical prediction that water and isopropyl acetate are pure component saddles, and the presence of two binary, nonreactive azeotropes, namely, isopropanol-isopropyl acetate and isopropanol-water.

Figure 8 also shows that residue curves calculated at $Da = 1$ closely follow the experimental data obtained. All the calculations performed using initial compositions very close to the isopropanol vertex of the diagram show a trend away from isopropanol, towards acetic acid. The experimental data are consistent with the predictions that (a) a single stable node at acetic acid exists at this reaction rate ($Da \approx 1$); (b) a pure

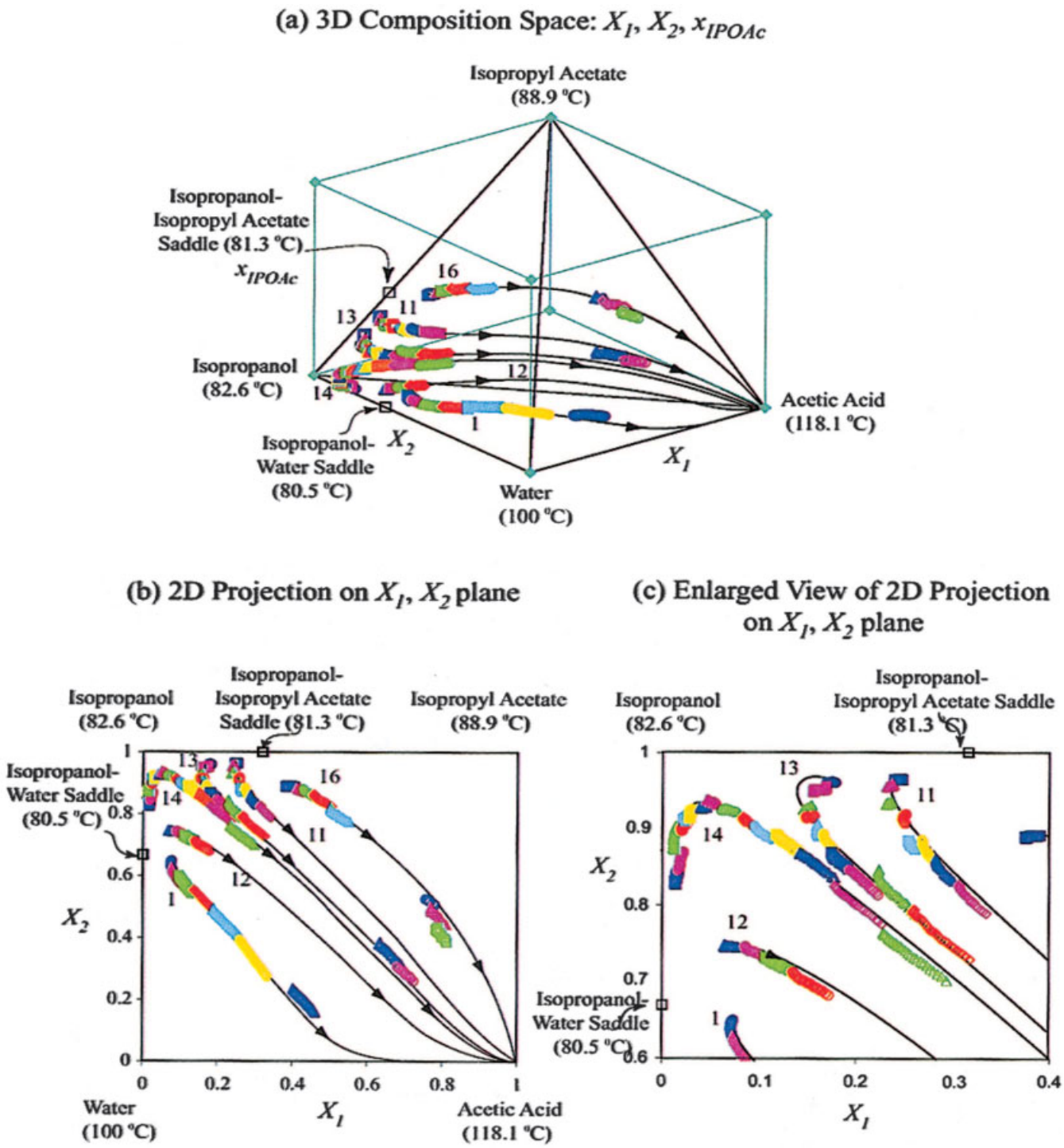

Figure 8. Experimental data at *Da* ≈ 1, (a) 3-D composition space, (b) 2-D projection, and (c) enlarged view of 2-D projection.

Solid lines represent the model calculations at $Da = 1$, and the arrows point in the direction of increasing time. Each experimental run is represented by a different color.

component saddle exists at isopropanol, and (c) there is no quaternary singular point. Table S-3 in the Supplementary Material provides the initial conditions for all the trajectories studied at $Da \approx 1$.

Damköhler number Da ≈ 2

Figure 9 shows the data collected by doubling the reaction rate, that is, at $Da \approx 2$, by doubling the amount of catalyst

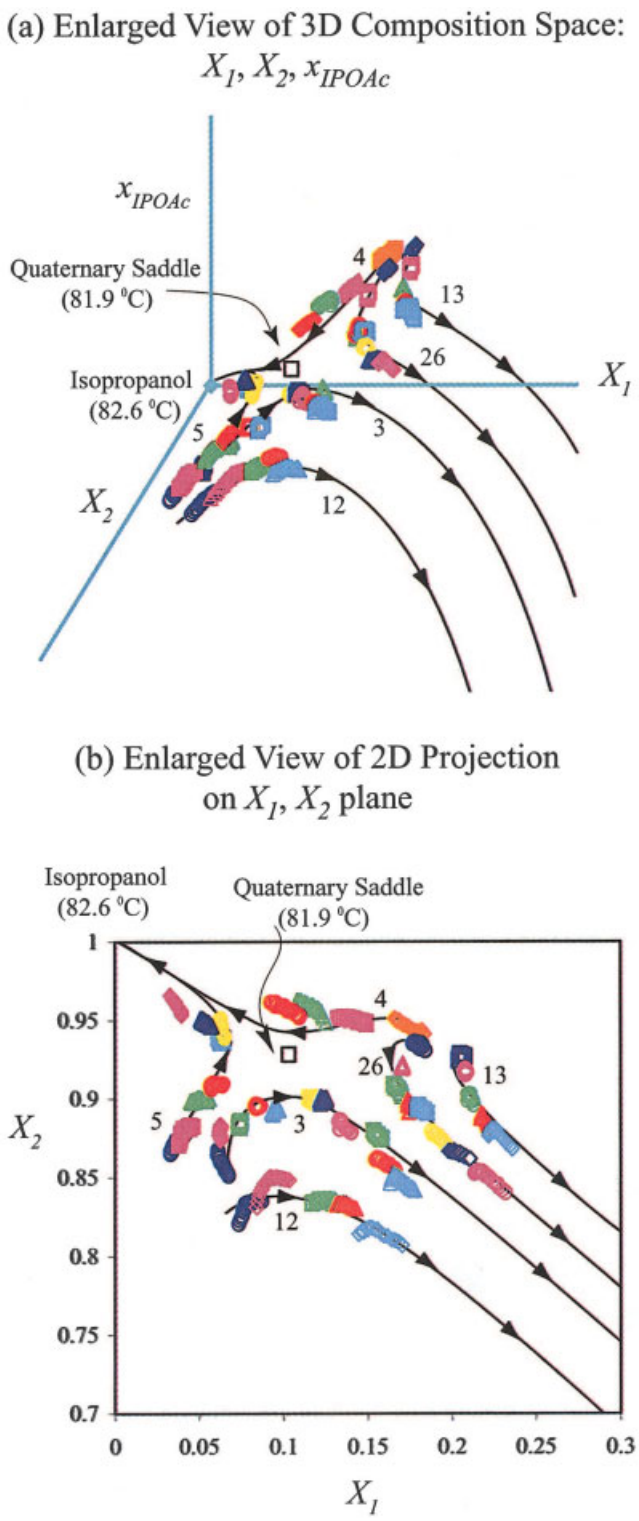

Figure 9. Experimental data at *Da* ≈ 2, (a) enlarged view of 3-D composition space, and (b) enlarged view of 2-D projection.

Solid lines represent the model calculations at $Da = 1.86$, and the arrows point in the direction of increasing time. Each experimental run is represented by a different color.

used, with the vapor rate and liquid holdup remaining the same as at the previous reaction rate (see Table 2). The set of features predicted at $Da \approx 2$ are different from those predicted for $Da \approx 1$. Calculations at $Da = 1$ predict the presence of a single stable node and all other singular points as saddles (binary and pure component saddles), whereas at $Da = 1.86$, the model predicts two stable nodes and a quaternary saddle, along with saddles at the remaining singular points (Figures 3 and 5). From the projection shown in Figure 9b, it is evident that there is a saddle type singular point. In this projection, the measurements show four separatrices, namely two moving towards the quaternary saddle, and two moving away from it (see dotted lines in Figure 5b). Trajectories 4 and 5 in Figure 9 show movement towards isopropanol, thus, indicating the possible existence of a stable node at isopropanol. For initial compositions that generate trajectories 13, 26, 3 and 12, the data show a trend towards acetic acid, indicating the presence of a possible second stable node at acetic acid. The presence of two stable nodes, thus, requires the presence of a distillation boundary, as shown in Figure 5b by the dotted lines. The exact composition of the saddle cannot be obtained experimentally, but the predicted value of the quaternary saddle is shown by the open square in Figure 9. The experimental data are consistent with the presence of a quaternary saddle, as predicted. The experimental data are also consistent with the prediction of acetic acid as a stable node, isopropanol as a stable node, and isopropanol-isopropyl acetate and isopropanol-water as binary saddles. At $Da \approx 2$ also, calculated residue curves closely follow the experimental data (Figure 9). Table S-4 in the Supplementary Material reports all the initial conditions studied for $Da \approx 2$.

The calculations shown by the solid lines in Figures 8 and 9 are for $Da = 1$ and $Da = 1.86$, respectively, and for an average initial molar liquid holdup $H_0 = 10$ mol and average vapor rate $V_0 = 0.105$ mol/min (over all the runs), using the LHHW kinetic rate model and the NRTL activity coefficient model.

Conclusions

The purpose of the experiment was to test the feasibility of products in the kinetic regime, for the stripping section of a reactive distillation column. The experiment was equivalent to the stripping section flash cascade, as proposed by Chadda et al. (2001). The reaction system studied was the esterification of acetic acid by isopropanol, heterogeneously catalyzed by Amberlyst-15, at atmospheric pressure. The behavior of the reaction system was studied at two reaction rates, corresponding to two Damköhler numbers in the bifurcation diagram. A comparison of the experimental data with theory at both the reaction rates, showed that the behavior of the reaction system in the kinetically-controlled reaction regime could be predicted very closely using the model developed and the feasibility theory. An experimental apparatus using Fourier transform infrared (FTIR) spectroscopy for measuring real-time liquid compositions in the reactor, was assembled. It should be noted that the model developed has an assumption of vapor-liquid equilibrium, and that there are no mass-transfer limitations present inside the catalyst. Nevertheless, the predictions from the model are able to explain the experimental results closely

Table 4. Initial Mole Fractions of Composition Trajectories (residue curves)

Trajectory No.	Mole Fractions				Transformed Compositions	
	x_{IPOH}	x_{IPOAc}	x_{H_2O}	x_{HOAc}	X_1	X_2
	Damköhler Number $Da \approx 1$					
16	0.550	0.340	0.071	0.039	0.379	0.890
11	0.723	0.241	0.027	0.009	0.250	0.964
13	0.787	0.173	0.033	0.007	0.180	0.960
14	0.817	0.010	0.170	0.003	0.013	0.827
12	0.715	0.032	0.220	0.033	0.065	0.747
1	0.600	0.048	0.326	0.026	0.074	0.648
	Damköhler Number $Da \approx 2$					
4	0.771	0.170	0.046	0.013	0.183	0.941
5	0.851	0.014	0.116	0.019	0.033	0.865
13	0.739	0.188	0.053	0.020	0.207	0.928
26	0.767	0.164	0.049	0.020	0.184	0.931
3	0.801	0.050	0.132	0.017	0.067	0.851
12	0.780	0.040	0.147	0.033	0.073	0.820

for the two reaction rates studied, namely, $Da \approx 1$ and $Da \approx 2$. The model and, hence, the feasibility theory can be used with increased confidence to make predictions of the feasible product compositions from a reactive distillation column.

Acknowledgments

We are grateful to the sponsors of the Process Design and Control Center, University of Massachusetts, Amherst. Financial support was provided by the National Science Foundation (Grant No. CTS-9613489). We would like to thank Wes Walker and Mark Parvlosky of ASI Applied Systems, Millersville, MD for their help. We would also like to thank Thomas Sweeney for preparing some of the illustrations.

Supplementary Material Available

Physical Property Data and Thermodynamic Data for the four components in isopropyl acetate reaction chemistry are reported in Tables PP-1, PP-2 and PP-3. Calibration Standards are reported in Table S-1. Table S-2 reports the compositions and the average and absolute errors in measurements in the Evaluation Samples taken. Initial conditions for the reaction rates studied, $Da \approx 1$ and $Da \approx 2$ are reported in Tables S-3 and S-4, respectively. Tables of experimental data for liquid compositions (Tables SL-1 to SL-12) and vapor compositions (Tables SV-1 to SV-12) for the isopropyl acetate system studied are available (54 runs for $Da \approx 1$, reported in Tables SL, SV 1–6, and 41 runs for $Da \approx 2$, reported in Tables SL, SV 7–12).

Notation

Variables

a_i = activity coefficient of component i
C_{pi}^L = liquid heat capacity of component i, kJ/mol K
c = number of components
Da = Damköhler number of the system, dimensionless
D = scaled Damköhler number, dimensionless
E = energy of activation, kJ/mol
g_{cat} = mass of wet Amberlyst-15 catalyst in g
H = liquid holdup in the still at any time, mol
ΔH_{fi}^o = heat of formation of component i at standard state, liquid state, 25°C, atmospheric pressure, kJ/mol
h^L, h^V = liquid and vapor enthalpy of the mixture, kJ/mol
ΔH_R = heat of reaction, kJ/mol
ΔH_i^V = heat of vaporization of component i at its boiling point, kJ/mol
K_D = dimerization constant for acetic acid, Pa^{-1}
K_{eq} = activity-based reaction equilibrium constant for isopropyl acetate system, dimensionless
K_i = adsorption equilibrium constant of component i, dimensionless
k_s = apparent forward reaction rate constant for surface reaction, mol reacted [mol H^+]$^{-1}$ min^{-1}
k_s^0 = apparent pre-exponential factor for surface reaction, mol reacted [mol H^+]$^{-1}$ min^{-1}
$k_{s,ref}$ = reference forward reaction rate constant for surface reaction, at 75°C, mol reacted [mol H^+]$^{-1}$ min^{-1}
M_{cat} = total moles of H^+ of catalyst, mol H^+
MW = molecular weight
P = total pressure, atm
$purity_i$ = purity of component i
Q = heating rate, kJ/min
$\Re$ = number of reactions
R = gas constant, 8.314×10^{-3} kJ/mol K
r = rate of reaction, mol reacted [mol of mixture]$^{-1}$ min^{-1}
T = temperature, °C
t = time, min
V = vapor rate at any time, mol/min
W = normalized catalyst concentration at time t, mol H^+/mol of mixture
w = mass fraction moisture content of the catalyst
X_1, X_2 = liquid phase transformed mole fractions 1 and 2
x_i = liquid phase mole fraction of component i
y_i = vapor phase mole fraction of component i
$\bar{y}_i$ = cup-mixed average vapor phase mole fraction of component i

Greek symbols

λ = latent heat of vaporization of mixture, kJ/mol
λ_i = latent heat of vaporization of component i at temperature T, kJ/mol
ν_i = stoichiometric coefficient of component i
$\nu_{T,j}$ = sum of stoichiometric coefficients of components i
ρ_i = density of component i, g/ml
ξ = warped time

Subscripts and superscripts

b = boiling point
c = critical property
i, k = component i, k
j = reaction j

0 = initial value
ref = reference state
sat = saturated state
V, L = vapor, liquid states
o = standard state

Literature Cited

Agreda, V. H., and L. R. Partin, Reactive Distillation Process for Production of Methyl Acetate. U.S. Patent 4,435,595 assigned to Eastman Kodak Company (1984).

Agreda, V. H., L. R. Partin, and W. H. Heise, "High Purity Methyl Acetate via Reactive Distillation," *Chem. Eng. Prog.,* **86**(2), 40 (1990).

ASI Applied Systems, "*ReactIR*™1000 and *ReactIR MP*™ *Mobile,* Reaction Analysis Systems: *ReactIR* Software, Version 2," 3rd ed., ASI Applied Systems, Millersville, MD (1997).

ASI Applied Systems, "*QuantIR*™ Software, Reaction Analysis Systems: Version 1.2," ASI Applied Systems, Millersville, MD (1997).

Barbosa, D., and M. F. Doherty, "The Simple Distillation of Homogeneous Reactive Mixtures," *Chem. Eng. Sci.,* **43,** 541 (1988a).

Barbosa, D., and M. F. Doherty, "Design and Minimum Reflux Calculations for Single-Feed Multicomponent Reactive Distillation Columns," *Chem. Eng. Sci.,* **43,** 1523 (1988b).

Bessling, B., M. Loning, A. Ohligschlager, G. Schembecker, and K. Sundmacher, "Investigations on the Synthesis of Methyl Acetate in a Heterogeneous Reactive Distillation Process," *Chem. Eng. Tech.,* **21,** 393 (1998).

Chadda, N., M. F. Malone, and M. F. Doherty, "Feasible Products for Kinetically Controlled Reactive Distillation of Ternary Mixtures," *AIChE J.,* **46,** 923 (2000).

Chadda, N., M. F. Malone, and M. F. Doherty, "Effect of Chemical Kinetics on Feasible Splits for Continuous Reactive Distillation," *AIChE J.,* **54,** 1010 (2001).

Chadda, N., M. F. Doherty, and M. F. Malone, "Feasibility and Synthesis of Hybrid Reactive Distillation Systems," *AIChE J.,* **48,** 2754 (2002).

Chiplunkar, M., "Experimental Study of Feasibility in Kinetically-Controlled Reactive Distillation," Masters Thesis, University of Massachusetts at Amherst (2002).

Dean, J. A., *Lange's Handbook of Chemistry,* 14th ed., McGraw-Hill, New York (1992).

Doedel, E., "AUTO: Software for Continuation and Bifurcation Problems in Ordinary Differential Equations," Dept. of Mathematics, California Institute of Technology, Pasadena (1986).

Doherty, M. F., and M. F. Malone, *Conceptual Design of Distillation Systems,* McGraw-Hill, New York (2001).

Espinosa, J., P. A. Aguirre, and G. A. Perez, "Product Composition Regions of Single-Feed Reactive Distillation Columns: Mixtures Containing Inerts," *Ind. Eng. Chem. Res.,* **34,** 853 (1995).

Fidkowski, Z. T., M. F. Doherty, and M. F. Malone, "Feasibility of Separations for Distillation of Non-Ideal Ternary Mixtures," *AIChE J.,* **39,** 1303 (1993).

Giessler, S., R. Y. Danilov, R. Y. Pisarenko, L. A. Serafimov, S. Hasebe, and I. Hashimoto, "Feasibility Study of Reactive Distillation Using the Analysis of the Statics," *Ind. Eng. Chem. Res.,* **37,** 4375 (1998).

Giessler, S., R. Y. Danilov, R. Y. Pisarenko, L. A. Serafimov, S. Hasebe, and I. Hashimoto, "Feasibility Separation Modes for Various Reactive Distillation Systems," *Ind. Eng. Chem. Res.,* **38,** 4860 (1999).

Gmehling, J., and U. Onken, *Vapor-Liquid Equilibrium Data Collection,* DECHEMA *Chemistry Data Series,* Frankfurt (1977).

Heese, F. P., M. E. Dry, and K. P. Möller, "Single Stage Synthesis of Diisopropyl Ether An Alternative Octane Enhancer for Lead-Free Petrol," *Catalysis Today,* **49,** 327 (1999).

Himmelblau, D., *Basic Principles and Calculations in Chemical Engineering,* 6th ed., Prentice Hall, NJ (1998).

IMSL Math/Library. FORTRAN *Subroutines for Mathematical Applications—IMSL Problem-solving Software Systems,* Version 1; IMSL, New York, 876 (1987).

Kipling, J. J., *Adsorption from Solutions of Non-Electrolytes,* Academic Press, New York (1965).

Kramer, R., *Chemometric Techniques for Quantitative Analysis,* Marcel Dekker, New York (1998).

Lee, L. S., and M. Z. Kuo, "Phase and Reaction Equilibria of Isopropanol-Acetic Acid-Isopropyl Acetate-Water System at 760 mm Hg," *Fluid Phase Equilib.,* **123,** 147 (1996).

Lee, J. W., S. Hauan, and A. W. Westerberg, "Graphical Methods for Reactive Distribution in a Reactive Distillation Column," *AIChE J.,* **46,** 1218 (2000).

Lide, D. R., *CRC Handbook of Chemistry and Physics,* 81st ed., CRC Press, New York (2000–2001).

Manning, J. M., "Kinetics and Feasibility of Reactive Distillation in Isopropyl Acetate Synthesis," Masters Thesis, University of Massachusetts at Amherst (1999).

Marek, J., and G. Standart, "Vapor-Liquid Equilibria in Mixtures Containing an Associating Substance, I. Equilibrium Relationships for System with an Associated Component," *Colln. Czech. Chem. Comm., Engl. Edn.,* **19,** 1074 (1954).

Martella, M., "The Effect of Heat of Reaction on Residue Curves for Simple Batch Reactive Distillation," Masters Thesis, University of Massachusetts at Amherst (1998).

Okasinski, M. J., and M. F. Doherty, "Thermodynamic Behavior of Reactive Azeotropes," *AIChE J.,* **43,** 2227 (1997).

Oyevaar, M. H., B. W. To, M. F. Doherty, and M. F. Malone, Process for Continuous Production of Carbonate Esters. U.S. Patent 6,093,842 (2000).

Reid, R. C., Prausnitz, J. M., and Sherwood, T. K., *The Properties of Gases and Liquids,* 3rd ed., McGraw-Hill, New York (1977).

Rev, E., "Reactive Distillation and Kinetic Azeotropy," *Ind. Eng. Chem. Res.,* **33,** 2174 (1993).

Solokhin, A. V., S. A. Blagov, L. A. Serafimov, and V. S. Timofeev, "Open Evaporation Processes Accompanied by Chemical Reaction in the Liquid Phase," *Theor. Found. Chem. Eng.,* **24**(2), 103 (1990).

Song, W., R. S. Huss, M. F. Doherty, and M. F. Malone, "Discovery of a Reactive Azeotrope," *Nature,* **388,** 561 (1997).

Song, W., G. Venimadhavan, J. M. Manning, M. F. Malone, and M. F. Doherty, "Measurement of Residue Curve Maps and Heterogeneous Kinetics in Methyl Acetate Synthesis," *Ind. Eng. Chem. Res.,* **37,** 1917 (1998).

Stichlmair, J. G., and J. R. Herguijeula, "Separation Regions and Processes of Zeotropic and Azeotropic Ternary Distillation," *AIChE J.,* **38,** 1523 (1992).

Sundmacher, K., L. K. Rihko, and U. Hoffmann, "Classification of Reactive Distillation Processes by Dimensionless Numbers," *Chem. Eng. Comm.,* **127,** 151 (1994).

Thiel, C., K. Sundmacher, and U. Hoffmann, "Residue Curve Maps for Heterogeneously Catalyzed Reactive Distillation of Fuel Ethers MTBE and TAME," *Chem. Eng. Sci.,* **52,** 993 (1997).

Ung, S., and M. F. Doherty, "Necessary and Sufficient Conditions for Reactive Azeotropes in Multireaction Mixtures," *AIChE J.,* **41,** 2383 (1995a).

Ung, S., and M. F. Doherty, "Calculation of Residue Curve Maps for Mixtures with Multiple Equilibrium Chemical Reactions," *Ind. Eng. Chem. Res.,* **34,** 3195 (1995b).

Venimadhavan, G., G. Buzad, M. F. Doherty, and M. F. Malone, "Effect of Kinetics on Residue Curve Maps for Reactive Distillation," *AIChE J.,* **40,** 1814 (1994). Correction: *AIChE J.,* **41,** 2613 (1995).

Venimadhavan, G., M. F. Malone, and M. F. Doherty, "Bifurcation Study of Kinetic Effects in Reactive Distillation," *AIChE J.,* **45,** 546 (1999).

Wahnschafft, O. M., J. W. Koehler, E. Blass, and A. W. Westerberg, "Product Composition Regions of Single-Feed Azeotropic Distillation Columns," *Ind. Eng. Chem. Res.,* **31,** 2345 (1992).

Xu, X., B. Zhu, H. Chen, and B. Bai, "Reactive Distillation," *Shiyou Huangong (Petrochemical Technology),* **14,** 480 (1985).

Appendix: General Model

Consider $\Re$ reactions taking place in the liquid-phase, with c components in the reaction chemistry. The reaction is heterogeneously catalyzed, and the catalyst concentration (W) is the ratio of the moles of H^+ to the molar liquid holdup of the mixture. The Langmuir-Hinshelwood-Hougen-Watson kinetic rate model is used to describe the reaction

chemistry. The rate of reaction r_j for the j^{th} reaction is given by

$$r_j = \frac{k_{s,j}\left(\prod_i^{Reactants} a_i^{\nu_{ij}} - \frac{1}{K_{eq,j}} \prod_i^{Products} a_i^{\nu_{ij}}\right) W}{\left(1 + \sum_{i=1}^{c} K_i a_i\right)^2} \quad \text{(A1)}$$

(Song et al., 1998; Manning, 1999), where $k_{s,j}$ is the apparent forward reaction rate constant, for the j^{th} reaction, W is the normalized catalyst concentration, a_i is the liquid-phase activity for species i, ν_{ij} is the stoichiometric coefficient of species i in reaction j, $K_{eq,j}$ is the reaction equilibrium constant for the j^{th} reaction, and K_i is the adsorption equilibrium constant for species i.

The component material balances for simple distillation for $i = 1, \ldots, c$ components can be written as

$$\frac{d(Hx_i)}{dt} = -Vy_i + H \sum_{j=1}^{\Re} \nu_{ij} r_j \quad \text{(A2)}$$

where x_i and y_i are liquid and vapor phase compositions, respectively, and H and V are molar liquid holdup and molar vapor flow rate, respectively.

Summing Eq. A2 for all species $i = 1, \ldots, c$ gives

$$\frac{dH}{dt} = -V + H \sum_{j=1}^{\Re} \nu_{T,j} r_j \quad \text{(A3)}$$

where

$$\nu_{T,j} = \sum_{i=1}^{c} \nu_{ij}$$

The normalized catalyst concentration W is defined as

$$W = \frac{M_{cat}}{H} \quad \text{(A4)}$$

In this derivation, it is assumed that the liquid holdup H decreases as a function of time, but the catalyst mass is unchanged and the catalyst is not deactivated. Thus, the catalyst composition changes as the holdup changes. At the initial time, $W = W_0$ and $H = H_0$.

Substituting Eqs. A1, A3, and A4 in Eq. A2 for species $i = 1, \ldots, c$ and, expressing time as warped time $d\xi = (V/H)dt$ gives

$$\frac{dx_i}{d\xi} = (x_i - y_i) + \frac{M_{cat}}{V} \sum_{j=1}^{\Re} (\nu_{ij} - x_i \nu_{T,j}) k_{s,j} \frac{\left(\prod_i^{Reactants} a_i^{\nu_{ij}} - \frac{1}{K_{eq,j}} \prod_i^{Products} a_i^{\nu_{ij}}\right)}{\left(1 + \sum_{i=1}^{c} K_i a_i\right)^2} \quad \text{(A5)}$$

Eq. A5 can be rewritten as

$$\frac{dx_i}{d\xi} = (x_i - y_i) + \left(\frac{H_0/V_0}{1/(k_{s,ref} W_0)}\right)\left(\frac{V_0}{V}\right) \sum_{j=1}^{\Re} (\nu_{ij} - x_i \nu_{T,j}) \times \left(\frac{k_{s,j}}{k_{s,ref}}\right) \frac{\left(\prod_i^{Reactants} a_i^{\nu_{ij}} - \frac{1}{K_{eq,j}} \prod_i^{Products} a_i^{\nu_{ij}}\right)}{\left(1 + \sum_{i=1}^{c} K_i a_i\right)^2} \quad \text{(A6)}$$

where, H_0 and V_0 are initial molar holdup and vapor rate, respectively, and $k_{s,ref}$ is the reference reaction rate constant at a reference temperature (75°C).

Defining the Damköhler number as

$$Da = \frac{H_0/V_0}{1/(k_{s,ref} W_0)} \quad \text{(A7)}$$

leads to

$$\frac{dx_i}{d\xi} = (x_i - y_i) + Da\left(\frac{V_0}{V}\right) \sum_{j=1}^{\Re} (\nu_{ij} - x_i \nu_{T,j}) \times \left(\frac{k_{s,j}}{k_{s,ref}}\right) \frac{\left(\prod_i^{Reactants} a_i^{\nu_{ij}} - \frac{1}{K_{eq,j}} \prod_i^{Products} a_i^{\nu_{ij}}\right)}{\left(1 + \sum_{i=1}^{c} K_i a_i\right)^2} \quad \text{(A8)}$$

Equation A8 becomes autonomous for a constant vapor rate policy, that is, $V = V_0$, whereas it is nonautonomous for a proportional vapor rate policy, $H/H_0 = V/V_0$.

Substituting, $d\xi = (V/H)dt$ in Eq. A3

$$\frac{dH}{d\xi} = -\frac{H}{V}\left[V - H \sum_{j=1}^{\Re} \nu_{T,j} r_j\right] \quad \text{(A9)}$$

Holdup H is a function of warped time $H/H_0 = f(\xi)$. Integration of Eq. A9, with $\nu_{T,j} = 0$ for all j gives

$$\frac{H}{H_0} = e^{-\xi} \tag{A10}$$

However, if any reaction is nonequimolar, the second term in brackets in Eq. A9 is nonzero. Thus, the term H/H_0, which is time-dependent, appears in the composition balances and they become nonautonomous equations. Variation of holdup as a function of time is then required to be known.

To find the variation of catalyst concentration with time, differentiate Eq. A4 with respect to time. Since, M_{cat} is constant, and H is a function of time, we find

$$\frac{dW}{dt} = \frac{d}{dt}\left(\frac{M_{cat}}{H}\right) = -\frac{M_{cat}}{H^2}\left[-V + H\sum_{j=1}^{\Re}\nu_{T,j}r_j\right] \tag{A11}$$

Substituting for warped time $d\xi = (V/H)dt$

$$\frac{dW}{d\xi} = W\left[1 - \frac{H}{V}\sum_{j=1}^{\Re}\nu_{T,j}r_j\right] \tag{A12}$$

Integrating Eq. A12 gives the catalyst composition W as a function of ξ. For example, for equimolar reaction chemistry, $\nu_{T,j} = 0$, and $dW/d\xi = W$, gives $W = W_0e^{\xi}$. There is an exponential increase in catalyst concentration with warped time.

Manuscript received Apr. 23, 2003, and revision received May 7, 2004.